

A Sterol-Binding Protein Integrates Endosomal Lipid Metabolism with TOR Signaling and Nitrogen Sensing

Carl J. Mousley,^{1,5,*} Peihua Yuan,¹ Naseem A. Gaur,² Kyle D. Trettin,¹ Aaron H. Nile,¹ Stephen J. Deminoff,³ Brian J. Dewar,⁴ Max Wolpert,¹ Jeffrey M. Macdonald,⁴ Paul K. Herman,³ Alan G. Hinnebusch,² and Vytas A. Bankaitis^{1,5,*}

¹Department of Cell and Developmental Biology, Lineberger Comprehensive Cancer Center, University of North Carolina School of Medicine, Chapel Hill, NC 27599-7090, USA

²Laboratory of Gene Regulation and Development, Eugene Shriver National Institute of Child Health and Human Development, National Institutes of Health, 6 Center Drive, Bethesda, MD 20892, USA

³Department of Molecular Genetics and Microbiology, The Ohio State University, Columbus, OH 43210, USA

⁴Department of Biomedical Engineering, University of North Carolina School of Medicine, Chapel Hill, NC 27599-7575, USA

⁵These authors contributed equally to this work

*Correspondence: mousley@email.unc.edu (C.J.M.), vytas@med.unc.edu (V.A.B.)

DOI 10.1016/j.cell.2011.12.026

SUMMARY

Kes1, and other oxysterol-binding protein superfamily members, are involved in membrane and lipid trafficking through trans-Golgi network (TGN) and endosomal systems. We demonstrate that Kes1 represents a sterol-regulated antagonist of TGN/endosomal phosphatidylinositol-4-phosphate signaling. This regulation modulates TOR activation by amino acids and dampens gene expression driven by Gcn4, the primary transcriptional activator of the general amino acid control regulon. Kes1-mediated repression of Gcn4 transcription factor activity is characterized by nonproductive Gcn4 binding to its target sequences, involves TGN/endosome-derived sphingolipid signaling, and requires activity of the cyclin-dependent kinase 8 (CDK8) module of the enigmatic “large Mediator” complex. These data describe a pathway by which Kes1 integrates lipid metabolism with TORC1 signaling and nitrogen sensing.

INTRODUCTION

Golgi and endosomes are dynamic organelles that combine physical properties of stable compartments with features consistent with a cycle of self-organized renewal and maturation (Glick and Nakano, 2009). These compartments are key membrane sorting stations and active sites of intracellular signaling. How Golgi/endosomal trafficking and signaling functions are coordinated is not understood, but a lipid signaling interface is an attractive mechanism given the established link between lipid metabolism and membrane trafficking in these compartments. Lipid-exchange proteins play important roles in coordinating lipid metabolism with the actions of protein

components of the membrane trafficking machinery in the trans-Golgi network (TGN) and the endosomal membrane system (Bankaitis et al., 2010; Graham and Burd, 2011).

Trafficking through the yeast TGN and endosomal systems is regulated by two lipid-exchange proteins that execute opposing activities (Cleves et al., 1991; Fang et al., 1996). The phosphatidylinositol (PtdIns)/phosphatidylcholine (PtdCho) transfer protein Sec14 is the pro-trafficking member of this pair. Sec14 acts as a coincidence sensor that couples PtdCho metabolism with PtdIns-4-phosphate production (PtdIns-4-P) (Schaaf et al., 2008; Bankaitis et al., 2010). PtdIns-4-P is an essential potentiator of membrane trafficking in the TGN/endosomal system (Hama et al., 1999; Rivas et al., 1999; Graham and Burd, 2011). The Sec14 antagonist is Kes1/Osh4, one of the seven yeast members of the oxysterol-binding protein (OSBP) superfamily (Fang et al., 1996). Kes1 dampens PtdIns-4-P signaling in TGN/endosomes (Li et al., 2002; Fairn et al., 2007; Stefan et al., 2011). Why cells engineer a Sec14/Kes1 “tug of war” into the TGN/endosomal trafficking design remains unclear.

Kes1 is a PtdIns-4-P and sterol-binding protein. PtdIns-4-P binding is a biologically important Kes1 activity and is required for Kes1 homing to TGN/endosomal membranes (Li et al., 2002). With regard to sterol binding, Kes1 is suggested to serve as a diffusible sterol carrier (Im et al., 2005; Schulz and Prinz, 2009). Carrier models are confronted with the rapid rate at which sterol shuttles between membranes via nonvesicular pathways, however (Mesmin and Maxfield, 2009), and measured rates for Kes1-mediated sterol transport in vitro are too slow to account for such rapid flux. New data argue that OSBPs have no role in sterol transport (Georgiev et al., 2011). This controversy underscores our lack of knowledge regarding how Kes1 translates sterol-binding activity to TGN/endosomal trafficking functions, and how Kes1 coordinates its dual PtdIns-4-P and sterol-binding activities.

Herein, we report that Kes1 integrates multiple aspects of lipid metabolism in distal stages of the secretory pathway with

TORC1 and nitrogen signaling. Kes1 couples TGN/endosomal sterol and PtdIns-4-P status with sphingolipid (SL) signaling from this endomembrane system. We show that Kes1-regulated SL-signaling in TGN/endosomal membranes attenuates activities of TORC1 and Gcn4, a primary transcription factor for control of amino acid homeostasis. Finally, we report that SL-regulated attenuation of Gcn4 activity requires a functional CDK8 module of the “large Mediator” complex, which regulates RNA polymerase II holoenzyme activity. These results introduce new conceptual frameworks for interpreting how Kes1, and other Kes1-like OSBPs, link membrane trafficking and lipid signaling with cell proliferation and transcriptional programs that respond to nitrogen stress.

RESULTS

Kes1 Defective in Sterol Binding Retains Biological Activity

Assignment of Kes1 as a TGN/endosomal trafficking “brake” derives from loss-of-function phenotypes recorded in complex genetic backgrounds (e.g., “bypass Sec14”) (Cleves et al., 1991; Fang et al., 1996; Li et al., 2002). The effects of a genuine trafficking brake should also be apparent in otherwise wild-type (WT) genetic backgrounds. Because Kes1 is a nonessential protein in vegetative cells, the function was probed in cells producing excess Kes1. The effects of acute elevations in Kes1 expression were monitored in WT yeast using an inducible system where *KES1* and *kes1* alleles of interest were placed under control of a doxycycline (Dox)-repressible promoter. Three Kes1 derivatives were expressed in parallel: (1) a biologically inactive *kes1*^{R236E,K242E,K243E} triple mutant (*kes1*^{3E}) unable to target to TGN/endosomal membranes because it is defective in PtdIns-4-P binding (Li et al., 2002); (2) the sterol-binding mutant *kes1*^{Y97F} (Im et al., 2005); and (3) a second putative sterol-binding mutant (*kes1*^{T185V}). The T₁₈₅V substitution, like Y₉₇F, is predicted to disrupt the ordered water chain that stabilizes sterol binding within the Kes1 lipid-binding pocket (Figure S1A available online).

Kes1 and its mutant derivatives were further characterized. [³H]-Cholesterol binding to Kes1 and *kes1*^{3E} was saturable (apparent $K_d \approx 0.5\text{--}0.8 \mu\text{M}$) and specific on the basis of its sensitivity to competition by unlabeled cholesterol (Figures S1B and S1C). In agreement with structural data (Im et al., 2005), the saturation binding data demonstrated both Kes1- and *kes1*^{3E}-bound [³H]-cholesterol in an ~1:1 stoichiometry ($B_{\max} = 1.2 \text{ pmol sterol bound/pmole protein}$). The Y₉₇F and T₁₈₅V substitutions each diminished specific cholesterol binding to the extent that saturation binding was not attainable. We estimate the binding affinities to be >70× weaker than those measured for Kes1 and *kes1*^{3E} (Figure S1C). Gel filtration and circular dichroism assays confirmed that *kes1*^{Y97F} and *kes1*^{T185V}, like Kes1, were well folded monomeric proteins (Figures S1D and S1E).

Introduction of *P_{DOX}::KES1*, *P_{DOX}::kes1^{Y97F}*, *P_{DOX}::kes1^{T185V}*, or *P_{DOX}::kes1^{3E}* vectors into yeast did not impair cell growth when the host yeast cells were cultured under noninducing conditions (in Dox-replete media). Induced Kes1 expression by Dox withdrawal severely inhibited cell growth, while *kes1*^{3E}

expression had no such detrimental effect (Figure 1). Unexpectedly, expression of the purportedly nonfunctional *kes1*^{Y97F} and *kes1*^{T185V} mutants also arrested growth of WT yeast (Figure 1A). The inducible *P_{DOX}* expression system elevated protein levels ~5-fold (relative to endogenous Kes1) following Dox withdrawal (Figure 1B), indicating that the inhibitory effects of *kes1*^{Y97F} and *kes1*^{T185V} were not results of excessive expression relative to Kes1 or *kes1*^{3E}. Toxicity of *kes1*^{Y97F} and *kes1*^{T185V} did not require strongly enhanced production. Yields of WT yeast transformants per unit DNA were reduced ~100-fold for YCp(*kes1*^{Y97F}) and YCp(*kes1*^{T185V}) plasmids relative to YCp(*KES1*) and YCp(*kes1*^{3E}). These YCp vectors drive only modest constitutive expression of the Kes1 derivatives (2-fold relative to endogenous Kes1) (Figure S1F). These data indicate that *kes1*^{Y97F} and *kes1*^{T185V} are more potent inhibitors of cell growth than is Kes1, a result that is incongruent with reports that loss of sterol binding inactivates Kes1 (Im et al., 2005; Schulz and Prinz, 2009). Although OSBPs are reported to function in concert with FFAT receptors (VAPs) (Stefan et al., 2011), Kes1-evoked arrest was indifferent to combinatorial ablation of VAP structural genes (*SCS2*, *SCS22*).

Kes1 is unique among the yeast OSBPs in its privileged interaction with Sec14-dependent pathways in TGN/endosomal trafficking (Fang et al., 1996). This specificity is reflected in the growth-inhibition assay. High-level expression of Hes1 (Osh5, the protein most similar to Kes1), the sterol-binding-defective *hes1*^{Y97F}, or Osh7 did not compromise cell proliferation.

Lipid Binding and Kes1 Association with TGN/Endosomes

Two lines of evidence show that sterol binding controls Kes1 association with TGN/endosomes. First, whereas Kes1-GFP adopted both diffuse cytosolic and punctate distributions in cells, *kes1*^{Y97F}-GFP localized predominantly to punctate structures (Figure 1C). These compartments were identified as TGN/endosomes because they load with FM4-64 under conditions where the tracer marks endocytic compartments (Figure 1D). Fractionation analyses also show increased *kes1*^{Y97F} membrane association (Figure S2A). In addition, our finding that challenge of cells with a sterol synthesis inhibitor (miconazole) provoked Kes1-GFP superrecruitment to punctate compartments loaded with FM4-64 (Figure 1E) also suggests that sterol binding releases Kes1 from TGN/endosomes.

Enhanced association of Kes1 and *kes1*^{Y97F} with TGN/endosomes also requires PtdIns-4-P-binding activity and robust Pik1-dependent PtdIns-4-P synthesis. Introduction of *kes1*^{3E} PtdIns-4-P-binding defects into the context of *kes1*^{Y97F} had the effect of (1) abrogating recruitment of the *kes1*^{Y97F} sterol-binding-defective mutant to TGN/endosomes (Figure 1G), and (2) relieving *kes1*^{Y97F}-mediated growth arrest (Figure 1H). Moreover, shift of *pik1-101^{ts}* yeast to 37°C, a condition nonpermissive for Pik1-mediated PtdIns-4-P production, released *kes1*^{Y97F}-GFP from TGN/endosomal membranes (Figure 1F).

Kes1 Restricts PtdIns-4-P Availability

Enhanced Kes1 recruitment to TGN/endosomes interfered with localization of the GOLPH3-GFP PtdIns-4-P sensor to this membrane system. In agreement with Wood et al. (2009),

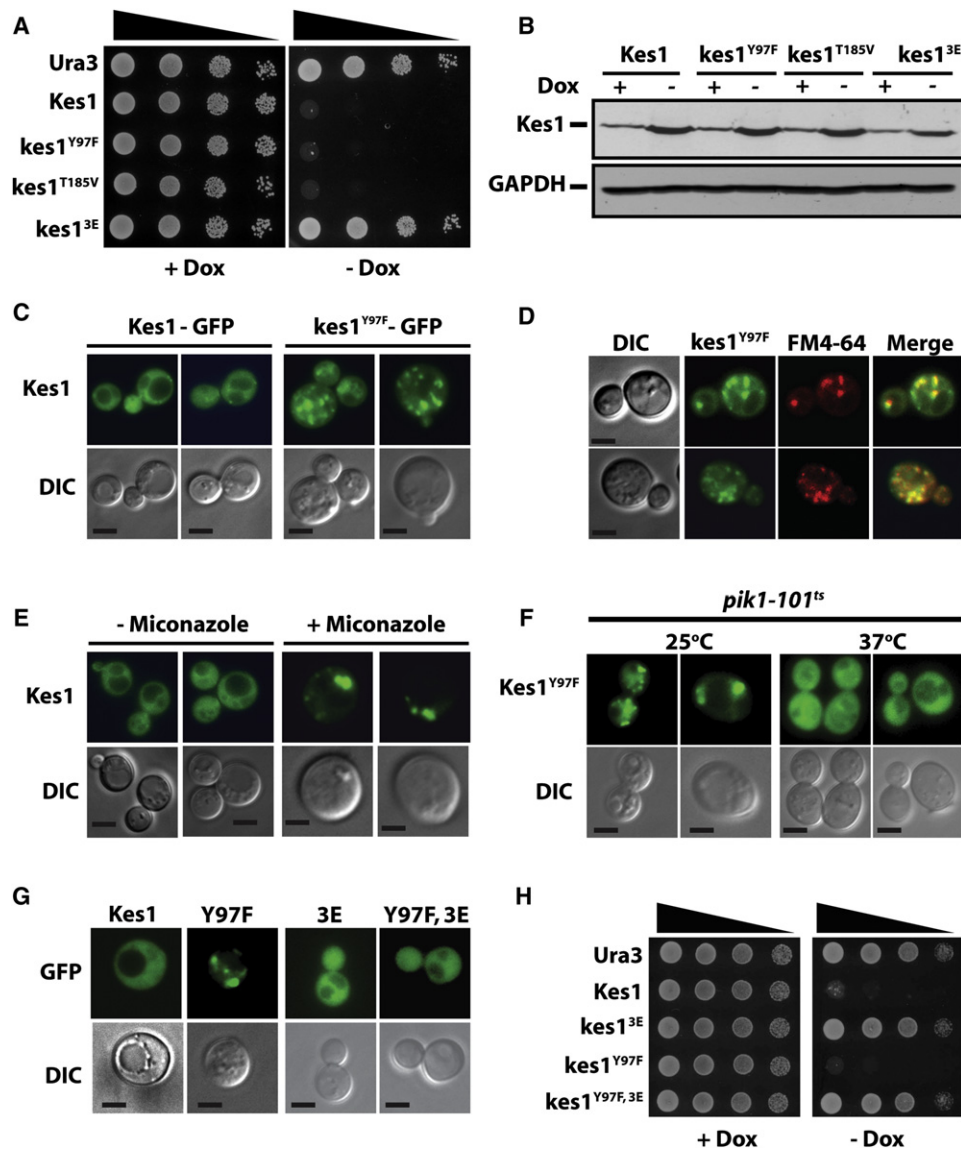


Figure 1. Sterol Binding Regulates Kes1 Activity

(A) WT yeast (CTY182) engineered for Dox-repressible expression of the indicated Kes1 derivatives were spotted in 10-fold dilution series on uracil-free media +/- Dox (10 μ g/ml) and incubated at 30°C.

(B) Lysates were prepared from the strains in (A) and normalized for total protein (10 μ g loaded), and Kes1 and GAPDH were visualized by immunoblotting.

(C) WT yeast expressing Kes1-GFP or kes1^{Y97F}-GFP were cultured to midlogarithmic growth phase in uracil-free medium at 30°C. GFP profiles are shown.

(D) WT yeast expressing kes1^{Y97F}-GFP were pulse-labeled with FM4-64 (10 μ M) for 10 min and poisoned with a 10 mM NaN₃/NaF cocktail. FM4-64, GFP, and merge profiles are shown with corresponding DIC image (bar = 5 μ m).

(E) WT yeast expressing Kes1-GFP were challenged with miconazole for 4 hr. GFP profiles are shown.

(F) *pik1-101^{ts}* cells expressing kes1^{Y97F}-GFP were cultured at 25°C and split; one culture was maintained at 25°C while the partner culture was shifted to 37°C for 1 hr prior to imaging.

(G) Profiles of GFP-tagged versions of the indicated Kes1 derivatives are shown with corresponding DIC images (bar = 5 μ m).

(H) WT yeast engineered for Dox-repressible expression of indicated Kes1 derivatives (or mock Ura3 control) were spotted in 10-fold dilution series on selective media with Dox (10 μ g/ml) as variable.

Also see Figures S1 and S2.

GOLPH3-GFP localized to TGN/endosomes in WT cells. This localization is PtdIns-4-P dependent, as indicated by release of GOLPH3-GFP upon Pik1 inactivation (Figure 2A). The GOLPH3-GFP chimera also distributed to TGN/endosomes

when WT cells bearing YCp(*P_{DOX}::KES1*) or YCp(*P_{DOX}::kes1^{Y97F}*) were cultured in noninducing medium (Figure 2B). Kes1/kes1^{Y97F} expression released a significant fraction of GOLPH3-GFP from TGN/endosomes (Figure 2B). Quantitative imaging

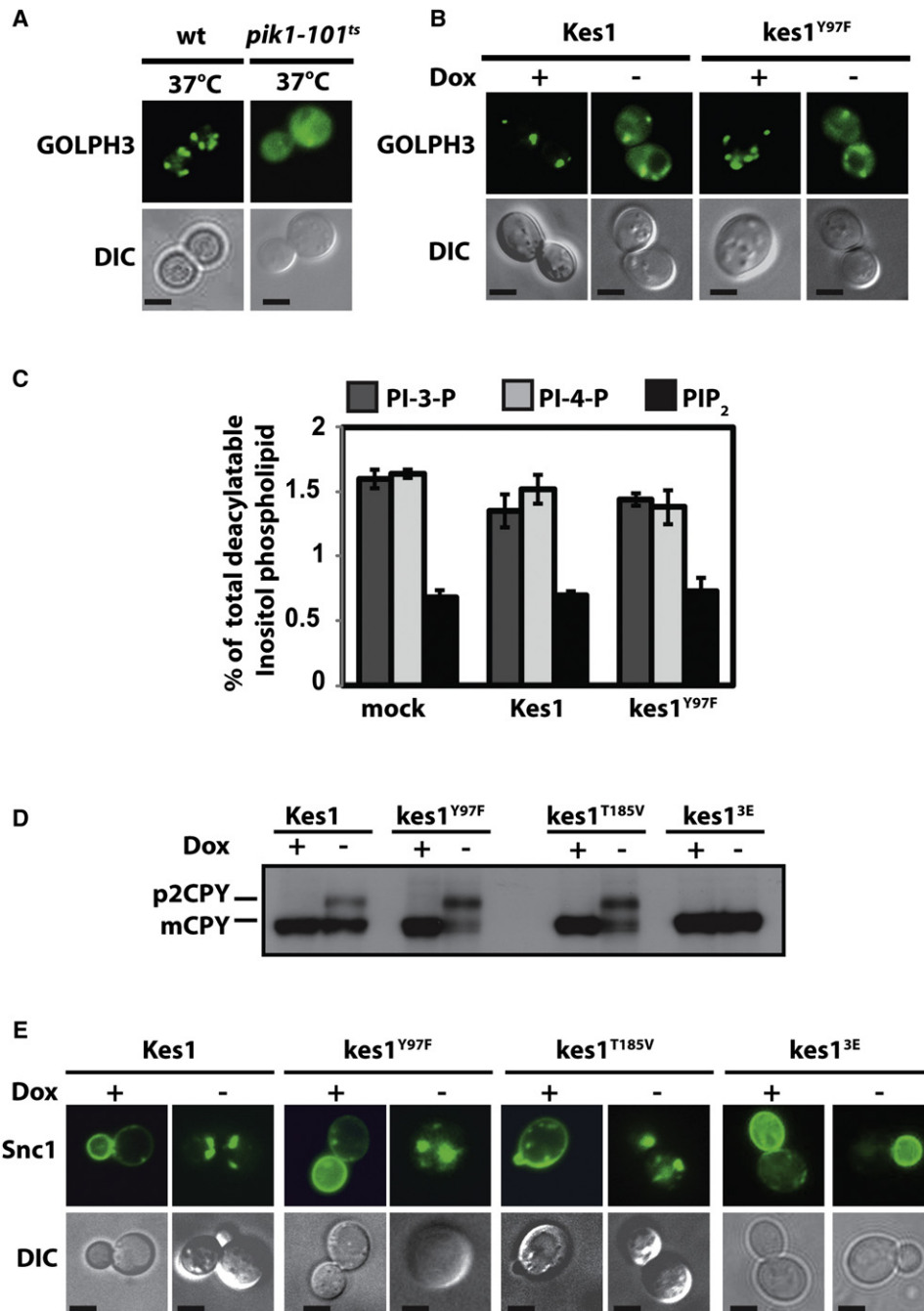


Figure 2. Kes1 and PtdIns-4-P Homeostasis

(A) WT and *pik1-101^{ts}* cells expressing GOLPH3-GFP were cultured in uracil-free medium at 25°C and shifted to 37°C for 60 min prior to imaging. Corresponding DIC images are shown at bottom (bar = 5 μm).

(B) WT yeast (CTY8-11C α) expressing GOLPH3-GFP and indicated Kes1 derivatives were incubated +/- Dox (10 μg/ml) for 18 hr. GOLPH3-GFP (top) and DIC image (bottom) profiles are shown (bar = 5 μm).

(C) WT yeast (CTY182) engineered for Dox-repressible expression of Kes1 derivatives were radiolabeled to steady state at 30°C with 20 μCi/ml [³H]-Ins +/- Dox as indicated. Fractional incorporation of [³H]-Ins into the deacylated PtdIns-3-P, PtdIns-4-P, and PtdIns(4,5)P₂ species is indicated (n = 4). Error bars represent standard deviation.

(D) WT yeast (CTY182) expressing the Kes1 derivatives were cultured +/- Dox. Cells were pulse-radiolabeled with [³⁵S]-amino acids (15 min). After 30 min of chase, immunoprecipitated CPY species were analyzed by SDS-PAGE and autoradiography. p2CPY and mCPY are indicated.

(E) WT yeast (CTY182) expressing Kes1 species (-Dox) and corresponding nonexpressing controls (+Dox), were examined for GFP-Snc1 distribution. DIC images are shown at bottom (bar = 5 μm).

Also see Figure S2.

analyses recorded 3-fold reductions in puncta fluorescence intensity relative to cytosol under those conditions ($n = 150$, $p = 0.0009$ and $p = 0.0003$). [^3H]-Inositol labeling showed no diminution of bulk PtdIns-4-P, or bulk levels of other phosphoinositides, in the face of Kes1/kes1^{Y97F} expression (Figure 2C). We conclude that Kes1 and kes1^{Y97F} sequester PtdIns-4-P without stimulating its degradation.

Kes1 Impairs Trafficking

The ability of Kes1 to bind PtdIns-4-P suggests that Kes1 interferes with interaction of this phosphoinositide with its prosecretory effectors. Several independent assays demonstrate that enhanced Kes1 activity impairs TGN/endosomal dynamics. Pulse-radiolabeling experiments show that carboxypeptidase Y (CPY) trafficking to the vacuole was inhibited by Kes1, kes1^{Y97F}, or kes1^{T185V} (Figure 2D). Trafficking of the Snc1 v-SNARE and the bulk endocytic tracer FM4-64 were also compromised by Kes1, kes1^{Y97F}, or kes1^{T185V} (Figure 2E). Normally, FM4-64 is internalized from the plasma membrane into endosomal compartments within 7.5 min of chase, and a significant fraction of the cell-associated FM4-64 is detected in the vacuole by that time point. The nonvacuolar FM4-64 pool chases from endosomes to vacuoles during the remainder of the time course (Figure S2C). FM4-64 trafficking was interrupted in cells with enhanced Kes1, kes1^{Y97F}, or kes1^{T185V} activities; >80% and >40% of cells presented solely punctate endosomal profiles after 15 and 30 min of chase. By 30 min, only 5% of the Kes1-, kes1^{Y97F}-, or kes1^{T185V}-expressing cells exhibited vacuolar labeling profiles (Figure S2C).

Trafficking defects were recorded for the general amino acid permease Gap1 (Figure S2D), and the defects in uptake of [^{35}S]-amino acids observed for yeast with enhanced Kes1/kes1^{Y97F} activity were also consistent with defects in amino acid permease trafficking to the plasma membrane (Figure S2B).

Kes1 Induces Autophagy

Kes1/kes1^{Y97F}-induced membrane trafficking defects notwithstanding, electron microscopy failed to record the typical accumulation of cargo-engorged TGN/endosomes. Instead, intravacuolar vesicles (diameter ~350 nm) were observed in >60% of cells expressing Kes1/kes1^{Y97F} (Figure 3A). These morphologies report that Kes1/kes1^{Y97F}-arrested cells were engaged in autophagy while bathed in nutrient-sufficient medium. Two other phenotypes support this diagnosis. First, we measured autophagic import from the cytoplasm of a modified alkaline phosphatase zymogen (Pho8 Δ 60) into the vacuole lumen, where Pho8 Δ 60 is activated (Noda et al., 1995). Pho8 Δ 60 activity was elevated 3.8- and 4.2-fold in the face of excess Kes1 and kes1^{Y97F} (Figure 3B). This enhancement was abrogated by *atg1 Δ* , an allele which blocks autophagy at an early stage (Figure S3A). Second, the Atg18 subunit of the preautophagosome was recruited to a juxtavacuolar location in Kes1/kes1^{Y97F}-arrested cells in a manner similar to that evoked by NH_4^+ starvation (Figures S3B and S3C).

Kes1/kes1^{Y97F}-mediated growth arrest is not accompanied by loss of viability, even after 20 days, indicating cell quiescence. Survival requires active autophagy, however. Arrested cells rapidly lose viability if they are incompetent for initiating auto-

phagy (*atg1 Δ* mutants) or if vacuolar protease activity is compromised (Figures S3D and S3E). Interestingly, Kes1/kes1^{Y97F}-arrested *atg1 Δ* cells accumulated cargo-engorged TGN/endosomes in the cytoplasm, while interference with vacuolar degradative functions resulted in membrane accretion in the vacuole lumen (Figure S3F). These observations indicate that the affected compartments are cleared by autophagy in Kes1/kes1^{Y97F}-arrested cells and degraded in the vacuole, which explains our initial failure to observe these structures by electron microscopy.

Kes1 Impairs Amino Acid Homeostasis

The autophagy phenotype suggested metabolic imbalances in cells with elevated Kes1 activity. A metabolomic signature for Kes1/kes1^{Y97F}-arrested yeast was established by profiling methanol-soluble small molecules by $^1\text{H-NMR}$ (Figure S4A). Unsupervised principal component analysis (PCA) deconvoluted the NMR spectra, and PCA score plots revealed informative variances in the first principal component (PC1) (Figure 3C). These variances clustered along compact regions of the PC1 axis and accounted for 51% of the total variance in the data set. The second principal component (PC2) further distinguished Kes1- from kes1^{Y97F}-expressing cells. Variances were again confined to narrow windows of the PC2 axis (Figure 3C). The discriminating methanol-soluble analytes were identified. Shown in Figure 3D is a comparison of selected metabolites from Kes1/kes1^{Y97F}-arrested cells and mock controls. Pools of 60% of the assignable amino acids were reduced at least 2-fold in the arrested cells. Most prominent were diminutions in Arg, Asn, Asp, Glu, Gln, Thr, and Trp pools (Figure S4B).

Amino Acid Resuscitation of Arrested Cells

A concentrated Asn/Glu/Gln/Arg (NEQR) cocktail rescued growth and amino acid pools of Kes1/kes1^{Y97F}-arrested cells (Figure 3E)—even though these cells are genetically NEQR prototrophs. Yet the trafficking defects associated with enhanced Kes1/kes1^{Y97F} activity remained unresolved. EM analyses demonstrated that NEQR-rescued cells, unlike Kes1/kes1^{Y97F}-arrested cells, accumulated cargo-engorged TGN/endosomes typically associated with trafficking defects through this system (Figure S4C).

The NEQR data demonstrate that Kes1/kes1^{Y97F}-induced arrest derives from amino acid deficiencies rather than from trafficking defects per se. The nature of the amino-acid-homeostatic problem is the focus of the remainder of this work. Several lines of evidence demonstrate that TORC1 activity is inversely proportional to potency of the Kes1 trafficking brake. First, phosphorylation of the TORC1 substrate Atg13 was reduced by Kes1/kes1^{Y97F} expression (Figure 3F). This effect was accompanied by phospho-eIF2 α accumulation—a hallmark of reduced TORC1 activity (Zaman et al., 2008). Second, genome content assays scored a G₁ block in Kes1/kes1^{Y97F}-arrested cells (Figure S4D). This block exhibits activated Rim15 signatures; a diagnosis of predisposal for entry into G₀. Third, *sec14-1^{ts}* yeast (harbor diminished activity for the protrafficking Sec14) were more rapamycin sensitive than isogenic WT strains. Increased rapamycin sensitivity was suppressed by *kes1 Δ* (Figure 3G). Furthermore, rapamycin-treated

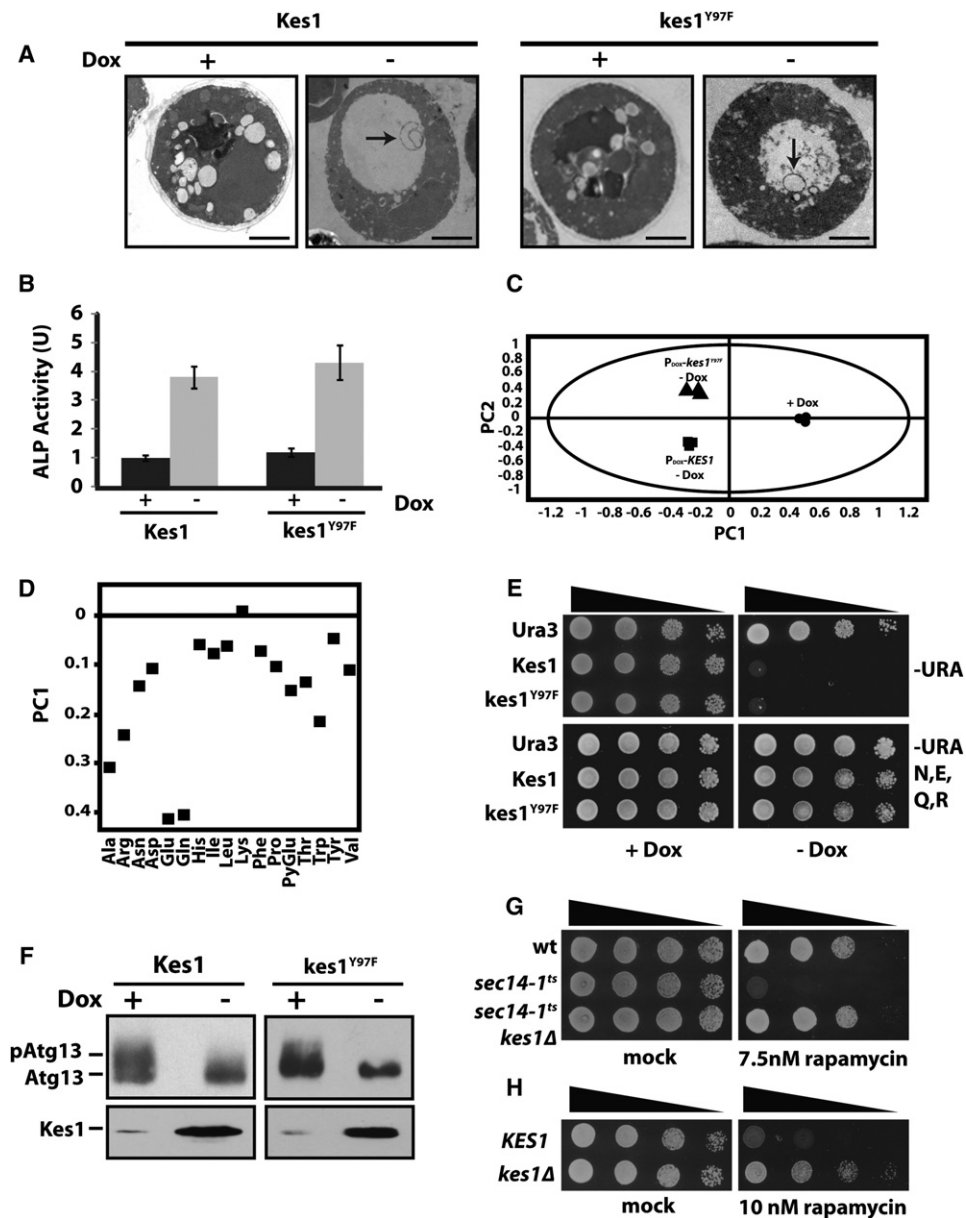


Figure 3. Kes1 and Amino Acid Homeostasis

(A) WT yeast cells (CTY182) producing Kes1 derivatives (– Dox) and corresponding nonexpressing controls (+ Dox; 10 μ g/ml) were analyzed by EM. Representative images are shown (bar = 1 μ m). Intravacuolar vesicular profiles (diameter \sim 350 nm) are highlighted by arrows.

(B) The ALP-expressing PHY2433 strain (TN124; Noda et al., 1995) was induced (– Dox), or not (+ Dox; 10 μ g/ml), for Kes1 or kes1^{Y97F} expression. Cultures were maintained at an OD_{600nm} < 0.2 throughout, harvested, and assayed for ALP activity. Error bars represent standard deviation.

(C) PCA scores plot distinguishing the ¹H-NMR metabolic profiles of WT yeast (CTY182) expressing Kes1 or kes1^{Y97F} (– Dox), or not (+ Dox).

(D) Targeted PCA of individual metabolites was performed for each condition. Reductions in Arg, Asn, Asp, Glu, Gln, Thr, and Trp pools were the major contribution to the variance between conditions of excess Kes1/kes1^{Y97F} and mock controls.

(E) WT yeast (CTY182) transformed with YCp(*URA3*), YCp(*P_{Dox}::KES1*), or YCp(*P_{Dox}::kes1^{Y97F}*) were spotted in 10-fold dilution series on media with Dox (10 μ g/ml) and amino acids (NEQR, 0.2% w/v).

(F) *atg13Δ* yeast cotransformed with YE(*P_{CUP1}::HA-ATG13*), and either YCp(*P_{Dox}::KES1*) or YCp(*P_{Dox}::kes1^{Y97F}*) was cultured in media containing 10 μ g/ml Dox. *KES1* or kes1^{Y97F} expression was induced for 7 hr (– Dox), or not (+ Dox; 10 μ g/ml), and cells were challenged with CuSO₄ (100 μ M for 1 hr) to induce HA-Atg13 expression. HA-Atg13 species were visualized by immunoblotting with anti-HA antibodies.

(G) WT (CTY182), *sec14-1^{ts}* (CTY1-1A), and *sec14-1^{ts} kes1Δ* (CTY159) yeast were spotted in 10-fold dilution series on media with or without 7.5 nM rapamycin and grown at 30°C.

(H) WT (CTY8-11C α) and *kes1Δ* (CTY2039) yeast were spotted in 10-fold dilution series on media with or without 10 nM rapamycin and grown at 37°C.

Also see Figures S3, S4, and S5.

kes1Δ cells accumulated less phospho-eIF2 α than did isogenic WT cells (Figure S5A), and both *sec14-1^{ts} kes1Δ*, and WT *kes1Δ* yeast showed increased rapamycin resistance relative to WT controls (Figures 3G and 3H). By contrast, a 2-fold elevation in *KES1* expression rendered a *sec14-1^{ts} cki1Δ* “bypass Sec14” mutant hypersensitive to rapamycin (Figure S5B). In all cases, the relative drug sensitivities reflected the magnitude of rapamycin-induced phospho-eIF2 α accumulation in these strains (see below).

Amino acids promote TORC1 signaling by potentiating Gtr1 and Gtr2 GTPase activities (Binda et al., 2009), and neither casamino acids nor NEQR revived growth of *Kes1/kes1^{Y97F}*-arrested *gtr1Δ* or *gtr2Δ* yeast (Figure S5C). NEQR resuscitated growth of *Kes1/kes1^{Y97F}*-arrested *spo14Δ* and *scs2Δ scs22Δ* mutants. These data demonstrate that neither phospholipase D nor FFAT receptors (VAPs) are required for the NEQR effect, but that Gtr-mediated activation of TORC1 is.

Kes1- and Gcn4-Dependent Transcriptional Regulation

The general amino acid control (GAAC) pathway is a major mechanism for amino acid homeostasis. The GAAC is activated by Gcn2-mediated phosphorylation of eIF2 α , a modification that reduces eIF2 α activity and promotes translation of the Gcn4 transcription factor ORF (Hinnebusch, 1997). The sensing component of the GAAC is engaged in *Kes1/kes1^{Y97F}*-arrested yeast, as evidenced by phospho-eIF2 α accumulation (Figures 4A and S5D). Yet downstream induction of the GAAC fails, as measured by induced *HIS4* and *ARG1* transcription (Figures 4B and S6A). In contrast, Gcn2 induced Gcn4-independent expression of *ARO9* and *ARO10* tryptophanase genes (Chen et al., 2009; Staschke et al., 2010) ~7-fold in *Kes1/kes1^{Y97F}*-arrested cells (Figure S6B). This induction likely contributed to the 50-fold reductions in Trp pools in those cells.

To assess Gcn4 status under conditions of enhanced *Kes1* activity, we employed a sensitized system where *sec14-1^{ts} cki1Δ* cells arrest in response to 2-fold elevations in *Kes1* level (Fang et al., 1996). *Kes1*-dependent increases in phospho-eIF2 α were reproduced in that genetic background (Figure S6C). However, translational derepression of *GCN4* was severely diminished (Figure S6D). The consequences are growth defects in minimal media supplemented with the His analog 3-aminotriazole (3-AT) (Figure S6E). Consistent data were also obtained from otherwise WT cells subjected to *Kes1/kes1^{Y97F}* growth arrest. Reduced Gcn4 accumulation was observed in those cells under conditions where Gcn4 production is normally induced by 3-AT (Figure 4C). Yet bypass of Gcn4 translational control (Gcn4^c) failed to activate the GAAC in *Kes1/kes1^{Y97F}*-arrested cells (Figures 4D and S6F), despite sustained Gcn4^c protein levels (Figure S5F). NEQR administration revived the GAAC in those cells (Figures 4E and S6G).

Inactivation of the GAAC without Increased Kes1 Expression

The data predicted that physiological levels of *Kes1* expression would silence the GAAC upon (1) enhanced *Kes1* recruitment to TGN/endosomes, or (2) imposition of TGN/endosomal traf-

ficking defects by reducing activities of proexocytic factors. *Kes1* load on TGN/endosomes was increased by challenging yeast with sub-growth-inhibitory levels of the sterol synthesis inhibitor miconazole. The intoxicated cells failed to respond appropriately to 3-AT challenge (Figure S7A).

The effects of *Kes1/kes1^{Y97F}* expression on GAAC activity were recapitulated in a mutant that expresses normal levels of *Kes1* but is compromised for two factors that promote TGN/endosomal trafficking (*sec14-1^{ts} tlg2Δ*) (Figure 4F). The quiescent GAAC was not only revived by *kes1Δ*, but was constitutively induced in *sec14-1^{ts} tlg2Δ kes1Δ* mutants (Figure 4F). This effect was not a general effect of “bypass Sec14” mutations, as *cki1Δ* failed to reactivate the GAAC in *sec14-1^{ts} tlg2Δ* yeast.

Kes1 and SL Metabolism

The GAAC defects observed in *sec14-1^{ts} tlg2Δ* cells were accompanied by elevated ceramide, sphingoid base, and sphingoid-base-phosphate mass (Figure S7B). *Kes1/kes1^{Y97F}*-arrested yeast similarly exhibited increases in dihydro- (DHC) and phytoceramide (PHC) mass, and dihydro- (DHS) and phytosphingosine (PHS) mass (Figure 5A). Increases were also measured for the sphingoid base phosphates (Figure 5A). Incorporation of *kes1Δ* into the *sec14-1^{ts} tlg2Δ* double mutant normalized intracellular ceramide, sphingoid base, and sphingoid-base-phosphate mass (Figure S7B). These lipidomics data suggest that SL metabolism links TGN/endosome trafficking status to nuclear transcriptional outcomes.

Sphingosine Feeding Compromises the GAAC

If *Kes1* extinguishes the GAAC via an SL-signaling mechanism, alterations in SL mass by means that do not affect cellular *Kes1* levels should also silence the GAAC. WT yeast were challenged with sub-growth-inhibitory levels of PHS. Histidine stress was superimposed on this condition by 3-AT challenge. While cell proliferation was unaffected by individual PHS or 3-AT challenge, both growth inhibition and blunting of the GAAC transcriptional response were elicited by dual challenge (Figures 5B, 5C, and S7C). The PHS-mediated inhibition of cell growth was apparent in the face of constitutive expression of Gcn4 (Figure 5D), and *HIS4* and *ARG1* transcription was strongly diminished under that condition as well (Figures 5E and S7D). TGN/endosomal trafficking was unperturbed under these conditions.

Sensitivity of the GAAC to PHS challenge requires *Kes1*, as *kes1Δ* cells exhibited enhanced resistance to PHS (Figure 5B). Gcn4-dependent *HIS4* and *ARG1* transcription was similarly resistant to dual PHS and 3-AT challenge in *kes1Δ* cells (Figures 5C and S7C). Finally, ectopic expression of the yeast Ypc1 phytoceramidase revived the GAAC in the face of *Kes1*- and PHS-challenge (Figures S7E and S7F). These data connect SL metabolism with GAAC activity and implicate ceramide as a key regulatory lipid.

Nonproductive Binding of Enhancer Elements by Gcn4

Chromatin immunoprecipitation experiments interrogated Gcn4 status on the *ARG1* promoter in vivo. Gcn4 binding at the *ARG1* upstream activation sequence (UAS) was induced

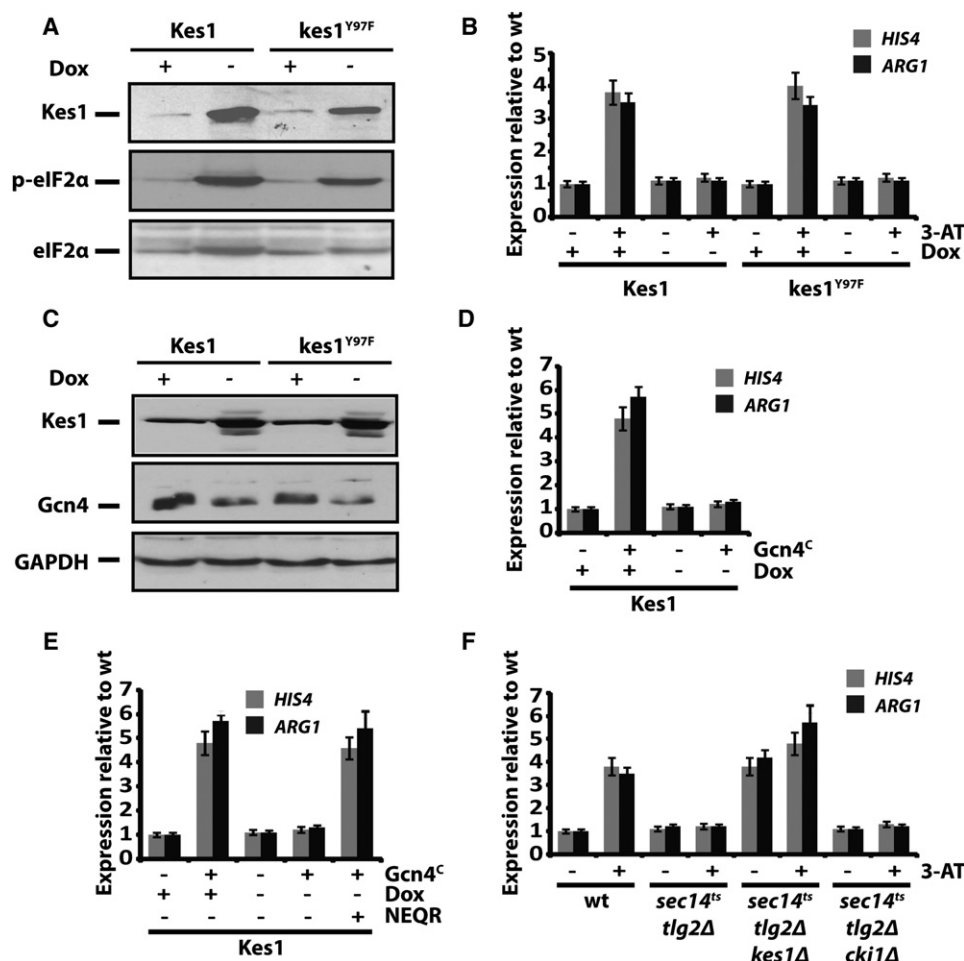


Figure 4. Kes1 Attenuates Gcn4-Dependent Activation of the General Amino Acid Control

(A) Lysates were prepared from paired cell cultures induced for Kes1 or *kes1*^{Y97F} expression (– Dox), or not (+ Dox; 10 μg/ml). Phospho-eIF2α, Kes1, and eIF2α were visualized by immunoblotting.

(B) Total RNA was prepared from cells (CTY8-11Cα) induced for Kes1 or *kes1*^{Y97F} expression (– Dox), or not (+ Dox), and challenged with 100 mM 3-AT for 2 hr to induce the GAAC. *HIS4*, *ARG1*, and *ACT1* expression were surveyed by RT-PCR. Error bars represent standard deviation.

(C) Gcn4, Kes1, and GAPDH were analyzed by immunoblotting of lysates prepared from WT cells (CTY8-11Cα) expressing Kes1 or *kes1*^{Y97F} (– Dox) or not (+ Dox). Cells were challenged with 100 mM 3-AT for 2 hr to induce the GAAC.

(D) Total RNA fractions were isolated from WT cells harboring YCp(*P*_{Dox}::*KES1*) and cotransformed with YCp(*TRP1*) or YCp(*GCN4*^C) cultured +/- Dox. *HIS4* and *ARG1* gene expression was surveyed by RT-PCR, and normalized to *ACT1* expression. Undiluted product and a 4-fold dilution of product were analyzed. Error bars represent standard deviation.

(E) The experiment is as in (D), with the modification that an NEQR cocktail (0.2% w/v) was added to a parallel culture induced for Kes1 expression. *HIS4*, *ARG1*, and *ACT1* expression were scored by RT-PCR. Error bars represent standard deviation.

(F) RT-PCR of GAAC target genes *ARG1* and *HIS4*, as well as *ACT1* control from total RNA fractions prepared from WT, *sec14-1^{ts} tlg2Δ*, *sec14-1^{ts} tlg2Δ kes1Δ*, or *sec14-1^{ts} tlg2Δ cki1Δ* cells shifted to 37°C for 2 hr to impose the strong *sec14-1^{ts} tlg2Δ*-associated TGN/endosomal trafficking block. Error bars represent standard deviation.

Also see Figure S6.

by 3-AT in both mock-treated yeast and yeast challenged with 15 μM PHS (Figure 6A). Enhanced RNA Polymerase II (Rpb3) occupancy evoked by 3-AT was dampened by PHS at the promoter and at 5' and 3' locations in *ARG1* coding sequences (Figure 6B). These results report only modest defects in the ability of UAS-bound Gcn4 to stimulate assembly of the preinitiation complex (PIC) at the *ARG1* promoter. Additional levels of regulation must be engaged downstream of PIC assembly

to account for the potent block of induced *ARG1* transcription by PHS.

Large-Mediator and GAAC Repression

Core Mediator is recruited to promoters by Gcn4, and it plays a key role in stimulating PIC assembly (Govind et al., 2005). The CDK8 module of the large Srb-Mediator complex, is implicated in transcriptional repression and in transcriptional

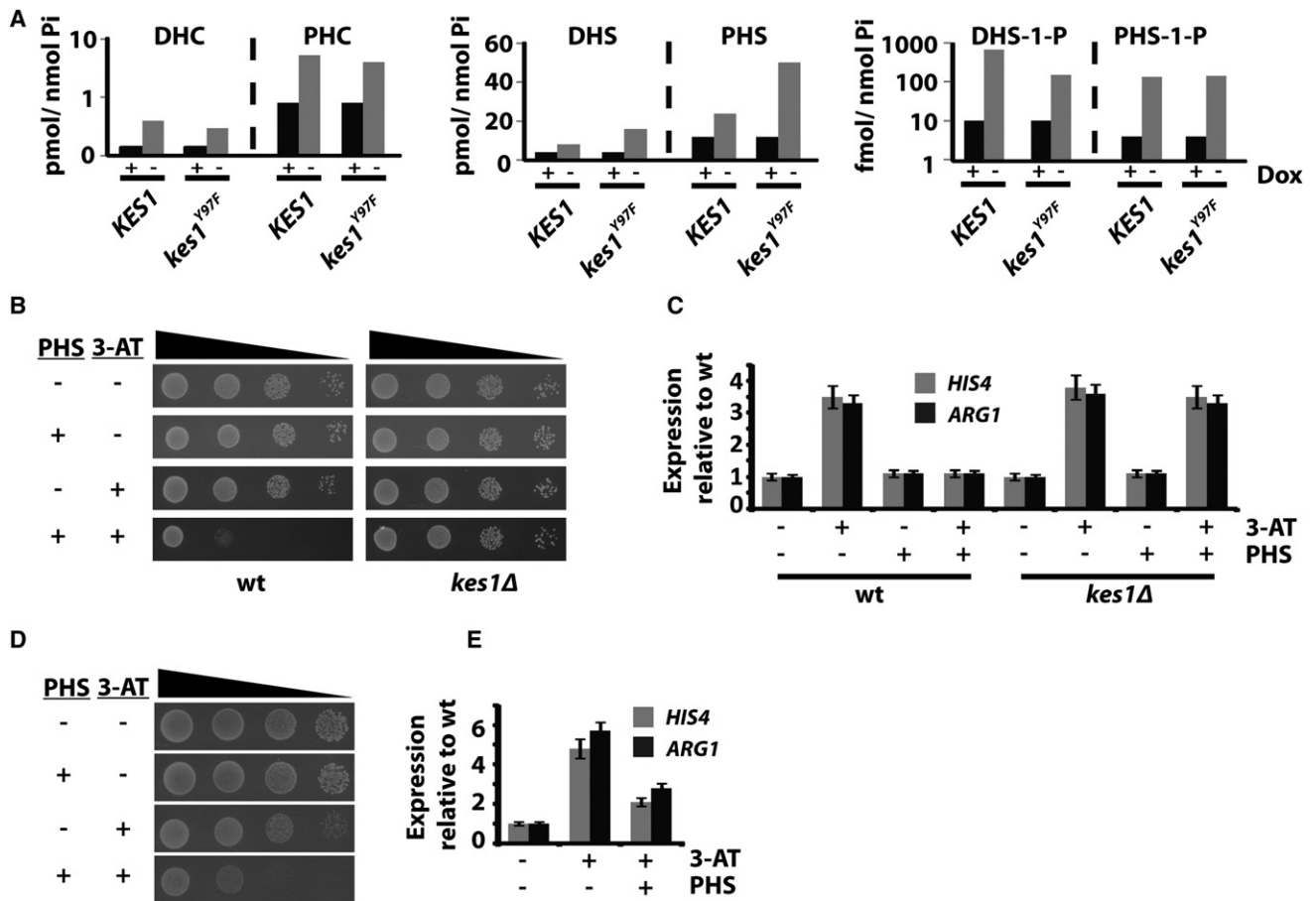


Figure 5. Spingolipids Inhibit the GAAC

(A) Quantitative lipidomics of DHC, PHC, DHS, PHS, DHS-1-P, and PHS-1-P in yeast (CTY182) as a function of Kes1 or Kes1^{Y97F} expression. Note the log₁₀ scale for the y axis.

(B) WT strain (CTY8-11C α) and a *kes1* Δ derivative were spotted in a 10-fold dilution series on synthetic-complete (SC) media and SC media with 7.5 μ M PHS, with 10 mM 3-AT, or both.

(C) Total RNA fractions were isolated from WT yeast either mock treated or grown in the presence of 7.5 μ M PHS for 2 hr. Cells were either mock-treated or challenged with 100 mM 3-AT for 2 hr to induce the GAAC. *HIS4*, *ARG1*, and *ACT1* expression were monitored by RT-PCR. Undiluted product and a 4-fold dilution of product were analyzed. Error bars represent standard deviation.

(D) WT yeast (CTY8-11C α) expressing Ura3 or Gcn4^c were spotted in a 10-fold dilution series on SC media and SC media with 7.5 μ M PHS, with 10 mM 3-AT, or both.

(E) Total RNA fractions were prepared from WT yeast expressing Ura3 or Gcn4^c +/- 15 μ M PHS for 2 hr. *HIS4* and *ARG1* expression were surveyed by RT-PCR and normalized to *ACT1* expression. Undiluted product and a 4-fold dilution of product were analyzed. Error bars represent standard deviation.

Also see Figure S7.

checkpoints (Myers and Kornberg, 2000; Hengartner et al., 1998; Taatjes, 2010). We found that Gcn4 inactivation in both Kes1- and PHS-intoxicated yeast required a functional Srb10, the cyclin-dependent kinase subunit of the CDK8 module. *srb10* Δ yeast were resistant to Kes1/*kes1*^{Y97F} arrest and to combinatorial PHS/3-AT challenge (Figures 6C and 6D). These phenotypes coincided with rejuvenated Gcn4-dependent *HIS4* and *ARG1* transcription (Figure 6E). The same results were obtained upon deletion of the structural genes encoding the other three components of the CDK8 module (Srb8, 9, and 11). Thus, the CDK8 module compromises the ability of Mediator to stimulate GAAC activation in response to altered TGN/endosomal SL signaling.

DISCUSSION

Herein, we demonstrate that Kes1 uses its sterol- and PtdIns-4-P-binding activities to integrate multiple pathways of endosomal lipid metabolism with the activity of TORC1-dependent proliferative pathways and transcriptional control of nitrogen signaling. This Kes1-regulated pathway provides mechanistic insights as to why GAAC activation by Gcn4 is sensitive to trafficking defects involving endosomal compartments (Mousley et al., 2008; Zhang et al., 2008). Finally, these findings generate conceptual frameworks for interpreting how Kes1, and other Kes1-like OSBPs, are integrated into eukaryotic cell physiology.

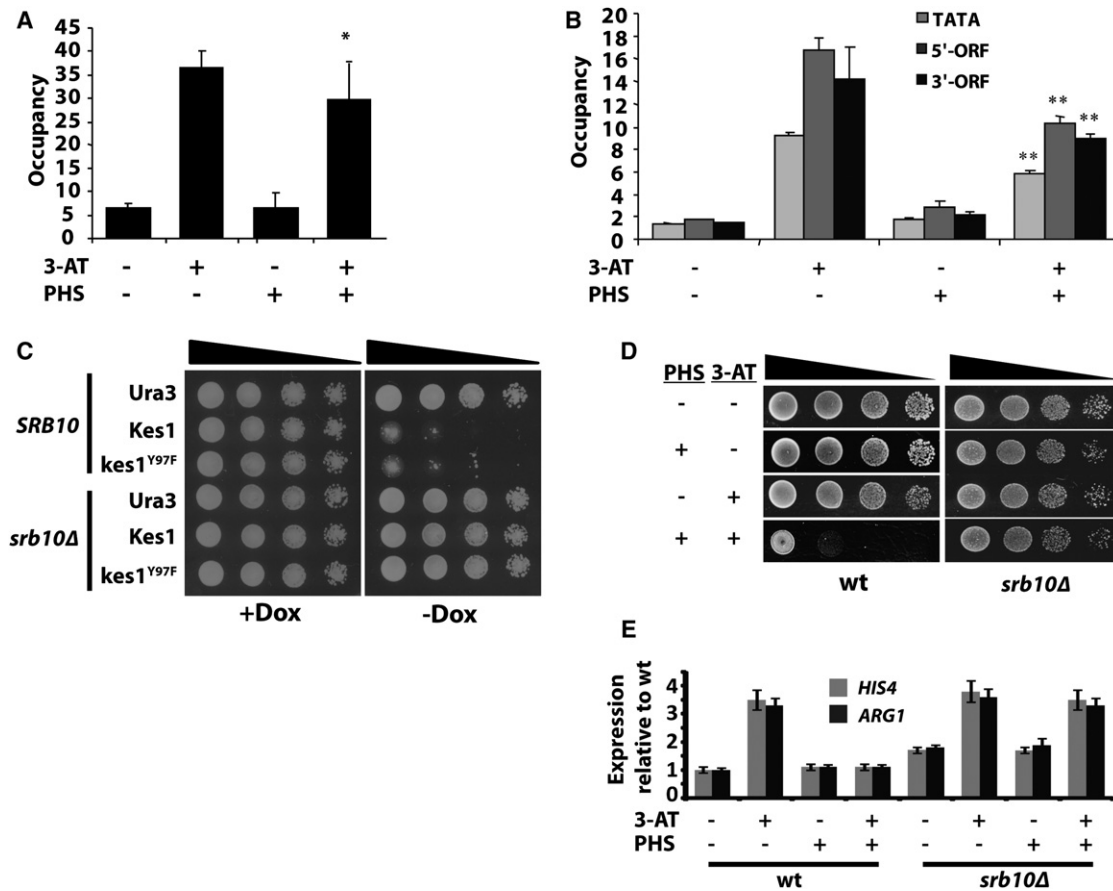


Figure 6. Gcn4 Binding to Target Genes and Mediator

(A and B) Cells were treated with PHS (15 μ M) for 2 hr prior to challenge with 3-AT (10 mM) for 30 min and perfused with formaldehyde. Sonicated chromatin was precipitated with antibodies against Gcn4 (A) or Rpb3 (B). DNA extracted from immunoprecipitates (ChIP) or starting chromatin (input) was PCR-amplified in the presence of [³²P]-dATP with primers for *ARG1* UAS (A), TATA element, or sequences from the 5' or 3' end of the *ARG1* coding sequences (B), and with primers for an intergenic chromosome V sequence (nonspecific control). PCR products were quantified by phosphorimaging. Ratios of *ARG1* ChIP-to-input signals were normalized against chromosome V control sequence ratios to yield occupancy values. Averages and standard errors from two PCR amplifications for each of two independent immunoprecipitates from two independent cultures are plotted. Error bars represent standard deviation.

(C) Isogenic WT (CTY1740) and *srb10Δ* yeast harboring YCp vectors for Dox-repressible expression of Kes1 were spotted in 10-fold dilutions series on media +/- Dox (10 μ g/ml) and incubated at 30°C.

(D) Isogenic WT (CTY1740) and *srb10Δ* yeast were spotted in a 10-fold dilution series on media with 7.5 μ M PHS, 10 mM 3-AT, or both 7.5 μ M PHS and 10 mM 3-AT.

(E) Isogenic WT (CTY1740) or *srb10Δ* yeast were either mock treated, or challenged with 15 μ M PHS for 2 hr. The cultures were challenged with 100 mM 3-AT for 2 hr to induce the GAAC. *HIS4*, *ARG1*, and *ACT1* expression was monitored by RT-PCR. Undiluted product and a 4-fold dilution of product were analyzed. Error bars represent standard deviation.

Kes1 Lipid Binding

The data identify Kes1 as a TGN/endosomal "trafficking brake" whose activity depends on PtdIns-4-P binding. The brake is attenuated by sterol binding which promotes Kes1 disengagement from PtdIns-4-P in TGN/endosomal membranes. We describe Kes1 as a sterol-regulated rheostat of TGN/endosomal PtdIns-4-P signaling. The interplay between sterol- and PtdIns-4-P binding regulates potency of Kes1-mediated inhibition of PtdIns-4-P-dependent trafficking through this endomembrane system. We cannot reconcile these results with conclusions that sterol-binding defects inactivate Kes1 (Im et al., 2005). Our data indicate that Kes1 couples TGN/endosomal sterol status

with efficacy of PtdIns-4-P signaling as a sterol sensor. Signaling circuits built on "tuning" principles do not require Kes1 to display the large capacities for sterol exchange demanded by nonvesicular sterol transfer models.

Kes1 and Nitrogen Signaling

A potent Kes1 TGN/endosomal membrane trafficking brake induces G₁/G₀ growth arrest associated with diminished TORC1 activity, induction of autophagy, and depleted amino acid pools. That amino acid homeostatic defects cause growth arrest is demonstrated by the Gtr GTPase dependence of NEQR-mediated resuscitation of cell proliferation, TORC1

activity, and proper amino acid homeostasis in cells with enhanced Kes1 activity. We write a chain of events where Kes1-evoked NH_4^+ starvation compromises TORC1 by attenuating amino acid stimulation of Gtr GTPases.

Asn is a critical component of the NEQR cocktail. We interpret that Asn essentiality reports NH_4^+ starvation as a key insult to Kes1-arrested cells because NEQR failed to rescue Kes1 arrest in *asp1 Δ* yeast. The Asp1 asparaginase produces Gln by transferring NH_2 from Asn to Glu. Gln is a key reservoir of biosynthetic NH_4^+ (Wise and Thompson, 2010), yet Gln supplementation failed to rescue Kes1-mediated growth arrest, suggesting that metabolic channeling of Asn is crucial. This concept might be of broad relevance, as the Gcn2-Atf4 pathway (Atf4 is mammalian Gcn4) supports Asn-dependent tumor survival (Ye et al., 2010).

Endosomal Signaling and Nuclear Outputs

Resuscitation of Kes1-arrested cells by NEQR occurred in the face of unresolved TGN/endosomal trafficking defects, signifying that the trafficking defects are, by themselves, insufficient to compromise cell proliferation. Growth arrest was driven by a TGN/endosomal SL-derived signal that dampens TORC1 and Gcn4 activities and leads to an insurmountable nitrogen deficit. The trafficking defects initiated the chain of events in two respects. First, they provided the initial insult to cellular nitrogen status. Amino acid and NH_4^+ permeases were not efficiently delivered to the plasma membrane under such conditions, thereby compromising nitrogen acquisition. Second, Kes1/*kes1*^{Y97F}-mediated trafficking defects increased SL-signal potency with downstream consequences, e.g., transcriptional downregulation of *Gap1* (3-fold) and of the major NH_4^+ -permease *Mep2* (8.5-fold).

Activation of autophagy, and proximal stages of the GAAC, indicated that Kes1-arrested yeast register nitrogen stress. Yet, the cells failed to execute a productive GAAC because *GCN4* mRNA translation was blunted. The translational defect might result from Gln deficiency. Gln is an indicator of nitrogen availability, and nitrogen starvation blocks translation of *GCN4* mRNA induced by phospho-eIF2 α (Grundmann et al., 2001). Kes1 signaling also inhibited Gcn4's activity as a transcription factor, recapitulating a phenotype we observed in *vps* mutants (Zhang et al., 2008). Hence, the transcriptional defects in *vps* mutants might also involve Kes1 signaling.

What SL biochemistry underlies the mechanism through which endosomal events influence nuclear Gcn4 activities? While the nature of the signal remains to be established, an SL-driven signaling pathway must negotiate the physical separation of these compartments. A diffusible enzyme (SL-activated kinase or phosphatase) might be activated on the endosomal surface and modify nuclear substrates that regulate Gcn4 activity. While the identities of nuclear effectors are unknown, the CDK module of large Mediator is an attractive candidate given that functional silencing of Gcn4 requires Srb10. Whether SLs stimulate Srb10 CDK activity is a key question. Gcn4 might represent the effector, as we observe an endosome-associated Gcn4 pool (N.A.G. and A.G.H., unpublished data). Epigenetic effects are also plausible as histone deacetylases are inhibited by sphingosine-1-P (Nitai et al., 2009).

Kes1 and Homeostatic Control

Why engineer a Sec14/Kes1 antagonism into the TGN/endosomal trafficking design? We propose that the Sec14/Kes1 tug of war sets the SL signaling output of a PtdIns-4-P/sterol-regulated endosomal compartment (Figure 7A). Appropriate tuning of signaling output is crucial, because the organelle couples membrane trafficking to local lipid metabolism and, subsequently, to global responses. The Kes1 brake on PtdIns-4-P signaling enhances production of bioactive SLs in an endosomal compartment monitored by homeostatic control systems (Figure 7B). Whereas such a design could be used in physiological contexts (see below), enhanced endosomal SL signaling exerts significant consequences for cell physiology, as manifested by the effects we document on TORC1 and GAAC signaling.

Although we focus on the GAAC, the nitrogen control response (NCR) is also silenced in Kes1-arrested cells. The NCR controls nitrogen acquisition via GATA transcription factor-regulated expression of amino acid and NH_4^+ permeases (e.g., *GAP1*, *MEP2*) (Zaman et al., 2008). NEQR supplementation, or Srb10 inactivation, also revives the NCR. NCR defects suggest a mechanism for transcriptional downregulation of *GAP1* and *MEP2* in Kes1-arrested cells.

Broader Implications for OSBPs?

Kes1-like proteins might be physiological modulators of cell proliferation programs. Loss of such activities will be scored under conditions where a trafficking brake needs to be imposed. In that regard, functional ablation of Kes1 compromises cell viability under starvation conditions, suggesting that loss of Kes1 activity hinders adjustment of endosomal lipid signaling by cells in response to nitrogen deprivation. The cardinal properties of Kes1-arrested yeast, like those of Sec14-deficient cells, conform to those of postmitotic cells. Perhaps privileged PtdIns transfer protein::OSBP pairs coevolved for fine-tuning systems that couple endosomal lipid signaling with cell proliferation. Such modalities could guide cell entry into postmitotic states or maintain postmitotic cell physiology. This concept raises possibilities for OSBPs flexibly coupling membrane trafficking flux and organelle maturation to the fine-tuning of transcriptional programs for organogenesis of tissues populated with postmitotic cells.

EXPERIMENTAL PROCEDURES

Yeast Strains and Media

Yeast strain genotypes and plasmids are listed in Tables S1 and S2. Yeast complex and synthetic complete media and yeast transformation methods were as described (Cleves et al., 1991; Schaaf et al., 2008). Fine chemicals were purchased from Sigma Chemical (St. Louis, MO, USA), and restriction enzymes were from New England Biolabs, Inc. (Ipswich, MA). YCp(*P_{DOX}::KES1*) transformants, and mutant derivatives thereof, were maintained in the presence of 10 $\mu\text{g}/\text{ml}$ Dox. To induce expression, cells were washed four times in ddH₂O and resuspended in fresh Dox-free media for a minimum of 8 hr. Amino acids (Asn, Glu, Gln, and Arg) were added at a final concentration of 0.2% (w/v). YCp(*P_{CUP1}-ATG13^{HA}*) expression was induced by the addition of 100 μM CuSO₄ for 1 hr.

Expression Vectors

To generate YCp(*P_{DOX}::KES1*), the *KES1* ORF was PCR amplified with oligonucleotides clamped with PmeI and PstI restriction sites at the 5' and 3' ends.

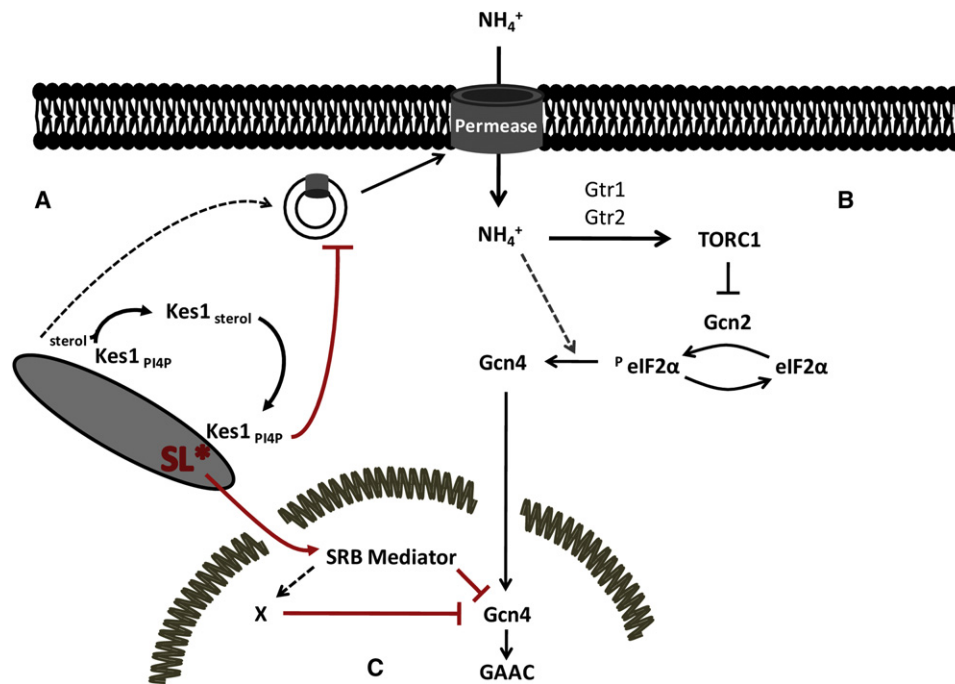


Figure 7. Integration of TGN/Endosomal Trafficking Flux to Transcriptional Competence of the Nitrogen Response

(A) Membrane trafficking through a signaling TGN/endosomal compartment is defined by Sec14-regulated production of PtdIns-4-P countered by Kes1-mediated PtdIns-4-P sequestration. Degree of sequestration is set by PtdIns-4-P-mediated recruitment of Kes1 to TGN/endosomal membranes, and released by binding of the membrane-bound Kes1 to active sterol.

(B) Kes1-mediated trafficking defects reduce efficiency of amino acid and NH₄⁺ permease delivery to the plasma membrane. The incipient nitrogen stress results in reduced TOR activity and engagement of the early stages of the GAAC (phosphorylation of eIF2 α). Efficiency of the terminal stages of the GAAC is determined by potency of Gcn4 antagonism levied by activity of the large SRB Mediator complex.

(C) Potency of a Kes1-mediated trafficking arrest/delay sets the amplitude of TGN/endosomal production of SL available for nuclear signaling. SL* denotes a sphingolipid with signaling power (e.g., ceramide) produced in TGN/endosomal compartments. The potency of SL* signaling is directly proportional to Kes1 activity, and inhibits transcription initiation/elongation of genes loaded with Gcn4 and RNA polymerase II via action of the CDK8 module of the large SRB Mediator complex. SL* signaling foils the GAAC and induces cells to enter a metabolically coherent quiescence with properties of postmitotic cell physiology.

The 1319 bp fragment was subcloned into pCM189 (Garí et al., 1997). Primer sequences are available from the authors by request.

Sterol Binding

The sterol:detergent micelle assay of Infante et al. (2007) was used to measure sterol binding with minor modification. Details are in the [Extended Experimental Procedures](#).

Fluorescence Microscopy

Cells grown at 30°C were incubated with a final concentration of 10 μ M FM4-64 (Molecular Probes) for 10 min. Labeling was stopped with 10 mM NaN₃/NaF. For GFP-Snc1 imaging, cells were cultured at 30°C. Images were collected with a Nikon E600 microscope equipped with a Princeton Instruments 512 X 512 back-illuminated frame-transfer CCD camera. MetaMorph (Universal Imaging Corp.) was used to capture images.

Transmission Electron Microscopy

Yeast were grown to midlogarithmic phase (OD_{600nm} = 0.3). Ten OD_{600nm} units of cells were isolated, and fixed in 3% glutaraldehyde. Cells were converted to spheroplasts with zymolyase, stained with 2% osmium tetroxide and 2% uranyl acetate, dehydrated in a 50%, 70%, 90% ethanol series, and washed in 100% ethanol and 100% acetone, respectively. Cells were embedded in Spurr's resin, and sections were prepared as described (Adamo et al., 2001) and visualized at 80 kV on an FEI Tecnai 12 electron microscope. Images were captured using Gatan micrograph 3.9.3 software.

Metabolic Labeling and Immunoprecipitation

Yeast were grown in minimal media lacking methionine and cysteine to mid-logarithmic phase (OD_{600nm} = 0.5) and radiolabeled with [³⁵S]-amino acids (Translabel; New England Nuclear; 100 μ Ci/ml). Chase was initiated by introduction of unlabeled methionine and cysteine (2 mM each, final concentration) for the specified time, and chase was terminated by addition of trichloroacetic acid (5% w/v final concentration). Immunoprecipitation of CPY with rabbit antiserum and resolution by SDS-PAGE and autoradiography were performed as previously described (Cleves et al., 1991; Schaaf et al., 2008).

Determination of LacZ Activity and RT-PCR

Yeast strains were transformed with plasmid p180 (Hinnebusch, 1985) and LacZ activity assayed (Mousley et al., 2008). For RT-PCR assays, total RNA was isolated from cells and 1 μ g was used to template reverse transcription to generate cDNA (20 μ l final volume). To analyze *HIS4*, *ARG1*, or *ACT1* expression, PCR was performed using 1 μ l of cDNA fraction as template and specific oligonucleotides as primers. Products were quantified with ImageQuant (GE Healthcare Life Science).

Autophagy Assays

Alkaline phosphatase assays that monitor delivery of a cytosolic Pho8 phosphatase reporter to the vacuole lumen by autophagy, and the subsequent proteolytic activation of this reporter in the vacuole, were performed as described (Stephan et al., 2009).

Sphingolipidomics

Ceramides and sphingoid bases were measured at the Lipidomics Shared Resource facility at the Medical University of South Carolina using normal-phase high-performance liquid chromatography coupled to atmospheric pressure chemical mass spectrometry (Bielawski et al., 2006). Neutral lipids were isolated from yeast extracts generated by pooling three independent cultures of each yeast strain that had been grown at 30°C. ESI/MS/MS analysis of ceramides and internal standards were performed on a Thermo Finnigan TSQ 7000 triple quadrupole mass spectrometer operating in a multiple-reaction-monitoring positive-ionization mode. Calibration curves for quantification were constructed by plotting peak area ratios of synthetic standards. Ceramides were normalized to total organic phosphate.

NMR Spectroscopy and Analysis

Small metabolites were extracted in 50% methanol and reconstituted in 0.5 mM trimethylsilyl-2,2',3,3'-tetradeuteropropionic acid in D₂O. ¹H NMR spectra were acquired at 16.4T with a Varian INOVA (700 MHz ¹H, Varian Instruments) equipped with 5 mm indirect cold probe and processed with ACD/1D NMR Manager (version 12.0; Advanced Chemistry Development, Inc., Toronto, ON, Canada). Spectra were phase and baseline corrected and referenced to the TSP peak to 0.00 ppm, and grouped spectra were data reduced to 250 bins using intelligent bucketing. Principal component analysis used SIMCA-P (version 11.0; Umetrics, Umea, Sweden) and Pareto scaling. Individual metabolites were quantified using Chenomx NMR Suite (version 5.1; Chenomx Inc., Edmonton, Canada), with TSP as concentration and chemical shift reference (Dewar et al., 2010). Details are described in the Extended Experimental Procedures.

Online Supplemental Information

Figure S1 describes properties of Kes1 sterol-binding mutants. Figure S2 describes effects of Kes1 and mutant Kes1 on TGN/endosomal trafficking. Figure S3 documents induction of autophagy by Kes1/kes1^{Y97F} expression and the role of autophagy in arrested cell viability. Figure S4 shows metabolomics profiling data. Figure S5 shows Kes1 modulation of TORC1 signaling. Figure S6 documents how Kes1/kes1^{Y97F} inhibits activation of the GAAC. Figure S7 shows that miconazole-evoked superrecruitment of Kes1 to TGN/endosomes inactivates the GAAC, that Kes1 regulates sphingolipid metabolism, and that sphingoid-base feeding inactivates the GAAC. Tables S1 and S2 list yeast strains and plasmids.

SUPPLEMENTAL INFORMATION

Supplemental Information includes Extended Experimental Procedures, seven figures, and two tables and can be found with this article online at doi:10.1016/j.cell.2011.12.026.

ACKNOWLEDGMENTS

This paper is dedicated to the memories of Christian Raetz and Eugene Kennedy. The work was supported by NIH grant GM44530 to V.A.B.; N.G. and A.G.H. were supported by the Intramural Research Program of the NIH; S.J.D. and P.K.H. by NIH grant GM65227 awarded to P.K.H.; and B.J.D. and J.M.M. by NIEHS T32EX007126 and GM075941. K.D.T. acknowledges support from the UNC William W. and Ida W. Taylor Honors Mentored Research Fellows Program. We thank Doug Cyr, Scott Moye Rowley, Chris Burd, and Dan Klionsky for strains and plasmids, Colin Stirling for CPY antibody, Chris Stefan, Scott Emr, and Maria Cardenas for discussions, and Lora Yanagisawa, Victoria Hewitt, and Robert Sons for comments on the manuscript. We acknowledge the UNC Lineberger Comprehensive Cancer Center Genome Analysis and Nucleic Acids Core facilities.

Received: October 15, 2010

Revised: October 13, 2011

Accepted: December 5, 2011

Published: February 16, 2012

REFERENCES

- Adamo, J., Moskow, J.J., Gladfelder, A.S., Viterbo, D., Lew, D.J., and Brennwald, P.J. (2001). Yeast Cdc42 functions at a late step in exocytosis, specifically during polarized growth of the emerging bud. *J. Cell Biol.* 155, 581–592.
- Bankaitis, V.A., Mousley, C.J., and Schaaf, G. (2010). The Sec14-superfamily and mechanisms for crosstalk between lipid metabolism and lipid signaling. *Trends Biochem. Sci.* 35, 150–160.
- Bielawski, J., Szulc, Z.M., Hannun, Y.A., and Bielawska, A. (2006). Simultaneous quantitative analysis of bioactive sphingolipids by high-performance liquid chromatography-tandem mass spectrometry. *Methods* 39, 82–91.
- Binda, M., Péli-Gulli, M.P., Bonfils, G., Panchaud, N., Urban, J., Sturgill, T.W., Loewith, R., and De Virgilio, C. (2009). The Vam6 GEF controls TORC1 by activating the EGO complex. *Mol. Cell* 35, 563–573.
- Chen, H., Huang, H., Li, X., Tong, S., Niu, L., and Teng, M. (2009). Crystallization and preliminary X-ray diffraction analysis of ARO9, an aromatic aminotransferase from *Saccharomyces cerevisiae*. *Protein Pept. Lett.* 16, 450–453.
- Cleves, A.E., McGee, T.P., Whitters, E.A., Champion, K.M., Aitken, J.R., Dowhan, W., Goebel, M., and Bankaitis, V.A. (1991). Mutations in the CDP-choline pathway for phospholipid biosynthesis bypass the requirement for an essential phospholipid transfer protein. *Cell* 64, 789–800.
- Dewar, B.J., Keshari, K., Jeffries, R.E., Dzeja, P., Graves, L.M., and Macdonald, J.M. (2010). Metabolic assessment of a novel chronic myelogenous leukemic cell line and an imatinib resistant subline by H NMR spectroscopy. *Metabolomics* 6, 439–450.
- Fair, G.D., Curwin, A.J., Stefan, C.J., and McMaster, C.R. (2007). The oxysterol binding protein Kes1p regulates Golgi apparatus phosphatidylinositol-4-phosphate function. *Proc. Natl. Acad. Sci. USA* 104, 15352–15357.
- Fang, M., Kearns, B.G., Gedvilaite, A., Kagiwada, S., Kearns, M., Fung, M.K.Y., and Bankaitis, V.A. (1996). Kes1p shares homology with human oxysterol binding protein and participates in a novel regulatory pathway for yeast Golgi-derived transport vesicle biogenesis. *EMBO J.* 15, 6447–6459.
- Gari, E., Piedrafita, L., Aldea, M., and Herrero, E. (1997). A set of vectors with a tetracycline-regulatable promoter system for modulated gene expression in *Saccharomyces cerevisiae*. *Yeast* 13, 837–848.
- Georgiev, A.G., Sullivan, D.P., Kersting, M.C., Dittman, J.S., Beh, C.T., and Menon, A.K. (2011). Osh proteins regulate membrane sterol organization but are not required for sterol movement between the ER and PM. *Traffic* 12, 1341–1355. 10.1111/j.1600-0854.2011.01234.x.
- Glick, B.S., and Nakano, A. (2009). Membrane traffic within the Golgi apparatus. *Annu. Rev. Cell Dev. Biol.* 25, 113–132.
- Govind, C.K., Yoon, S., Qiu, H., Govind, S., and Hinnebusch, A.G. (2005). Simultaneous recruitment of coactivators by Gcn4p stimulates multiple steps of transcription in vivo. *Mol. Cell Biol.* 25, 5626–5638.
- Graham, T.R., and Burd, C.G. (2011). Coordination of Golgi functions by phosphatidylinositol 4-kinases. *Trends Cell Biol.* 21, 113–121.
- Grundmann, O., Mösch, H.U., and Braus, G.H. (2001). Repression of GCN4 mRNA translation by nitrogen starvation in *Saccharomyces cerevisiae*. *J. Biol. Chem.* 276, 25661–25671.
- Hama, H., Schnieders, E.A., Thorner, J., Takemoto, J.Y., and DeWald, D.B. (1999). Direct involvement of phosphatidylinositol 4-phosphate in secretion in the yeast *Saccharomyces cerevisiae*. *J. Biol. Chem.* 274, 34294–34300.
- Hengartner, C.J., Myer, V.E., Liao, S.-M., Wilson, C.J., Koh, S.S., and Young, R.A. (1998). Temporal regulation of RNA polymerase II by Srb10 and Kin28 cyclin-dependent kinases. *Mol. Cell* 2, 43–53.
- Hinnebusch, A.G. (1985). A hierarchy of trans-acting factors modulates translation of an activator of amino acid biosynthetic genes in *Saccharomyces cerevisiae*. *Mol. Cell Biol.* 5, 2349–2360.
- Hinnebusch, A.G. (1997). Translational regulation of yeast GCN4. A window on factors that control initiator-tRNA binding to the ribosome. *J. Biol. Chem.* 272, 21661–21664.

- Im, Y.J., Raychaudhuri, S., Prinz, W.A., and Hurley, J.H. (2005). Structural mechanism for sterol sensing and transport by OSBP-related proteins. *Nature* **437**, 154–158.
- Infante, R.E., Abi-Mosleh, L., Radhakrishnan, A., Dale, J.D., Brown, M.S., and Goldstein, J.L. (2007). Purified NPC1 protein. 1. Binding of cholesterol and oxysterols to a 1278-amino acid membrane protein. *J. Biol. Chem.* **283**, 1052–1063.
- Li, X.M.P., Rivas, M.P., Fang, M., Marchena, J., Mehrotra, B., Chaudhary, A., Feng, L., Prestwich, G.D., and Bankaitis, V.A. (2002). Analysis of oxysterol binding protein homologue Kes1p function in regulation of Sec14p-dependent protein transport from the yeast Golgi complex. *J. Cell Biol.* **157**, 63–77.
- Mesmin, B., and Maxfield, F.R. (2009). Intracellular sterol dynamics. *Biochim. Biophys. Acta* **1791**, 636–645.
- Mousley, C.J., Tyeryar, K., Ile, K.E., Schaaf, G., Brost, R.L., Boone, C., Guan, X., Wenk, M.R., and Bankaitis, V.A. (2008). Trans-Golgi network and endosome dynamics connect ceramide homeostasis with regulation of the unfolded protein response and TOR signaling in yeast. *Mol. Biol. Cell* **19**, 4785–4803.
- Myers, L.C., and Kornberg, R.D. (2000). Mediator of transcriptional regulation. *Annu. Rev. Biochem.* **69**, 729–749.
- Noda, T., Matsuura, A., Wada, Y., and Ohsumi, Y. (1995). Novel system for monitoring autophagy in the yeast *Saccharomyces cerevisiae*. *Biochem. Biophys. Res. Commun.* **210**, 126–132.
- Rivas, M.P., Kearns, B.G., Xie, Z., Guo, S., Sekar, M.C., Hosaka, K., Kagiwada, S., York, J.D., and Bankaitis, V.A. (1999). Pleiotropic alterations in lipid metabolism in yeast *sac1* mutants: relationship to “bypass Sec14p” and inositol auxotrophy. *Mol. Biol. Cell* **10**, 2235–2250.
- Schaaf, G., Ortlund, E., Tyeryar, K., Mousley, C., Ile, K., Woolls, M., Garrett, T., Raetz, C.R.H., Redinbo, M., and Bankaitis, V.A. (2008). Functional anatomy of phospholipid binding and regulation of phosphoinositide homeostasis by proteins of the Sec14 superfamily. *Mol. Cell* **29**, 191–206.
- Schulz, T.A., and Prinz, W.A. (2009). Sterol transport in yeast and the oxysterol binding protein homologue (OSH) family. *Biochim. Biophys. Acta* **1771**, 769–780.
- Staschke, K.A., Dey, S., Zaborske, J.M., Palam, L.R., McClintick, J.N., Pan, T., Edenberg, H.J., and Wek, R.C. (2010). Integration of general amino acid control and target of rapamycin (TOR) regulatory pathways in nitrogen assimilation in yeast. *J. Biol. Chem.* **285**, 16893–16911.
- Stephan, J.S., Yeh, Y.Y., Ramachandran, V., Deminoff, S.J., and Herman, P.K. (2009). The Tor and PKA signaling pathways independently target the Atg1/Atg13 protein kinase complex to control autophagy. *Proc. Natl. Acad. Sci. USA* **106**, 17049–17054.
- Stefan, C.J., Manford, A.G., Baird, D., Yamada-Hanff, J., Mao, Y., and Emr, S.D. (2011). Osh proteins regulate phosphoinositide metabolism at ER-plasma membrane contact sites. *Cell* **144**, 389–401.
- Taatjes, D.J. (2010). The human Mediator complex: a versatile, genome-wide regulator of transcription. *Trends Biochem. Sci.* **35**, 315–322.
- Wise, D.R., and Thompson, C.B. (2010). Glutamine addiction: a new therapeutic target in cancer. *Trends Biochem. Sci.* **35**, 427–433.
- Wood, C.S., Schmitz, K.R., Bessman, N.J., Setty, T.G., Ferguson, K.M., and Burd, C.G. (2009). PtdIns4P recognition by Vps74/GOLPH3 links PtdIns 4-kinase signaling to retrograde Golgi trafficking. *J. Cell Biol.* **187**, 967–975.
- Ye, J., Kumanova, M., Hart, L.S., Sloane, K., Zhang, H., De Panis, D.N., Bobrovnikova-Marjon, E., Diehl, J.A., Ron, D., and Koumenis, C. (2010). The GCN2-ATF4 pathway is critical for tumour cell survival and proliferation in response to nutrient deprivation. *EMBO J.* **29**, 2082–2096.
- Zaman, S., Lippman, S.I., Zhao, X., and Broach, J.R. (2008). How *Saccharomyces* responds to nutrients. *Annu. Rev. Genet.* **42**, 27–81.
- Zhang, F., Gaur, N.A., Hasek, J., Kim, S.J., Qiu, H., Swanson, M.J., and Hinnebusch, A.G. (2008). Disrupting vesicular trafficking at the endosome attenuates transcriptional activation by Gcn4. *Mol. Cell. Biol.* **28**, 6796–6818.